Mechanochemical Preparation of Alumina-Ceria

Jirátová, Květa
2015

MECHANOCHEMICAL PREPARATION OF ALUMINA-CERIA

Jirátová K.[1], Spojakina A.[2], Tyuliev G.[2], Balabánová J.[1], Kaluža L.[1], Palcheva R.[2]

[1]*Institute of Chemical Process Fundamentals of the CAS, v.v.i, Prague, Czech Republic*
[2]*Institute of Catalysis, BAS, Sofia, Bulgaria*
jiratova@icpf.cas.cz

Ceria containing catalysts play an essential role in heterogeneous catalytic processes. However, ceria shows poor thermal stability and low specific surface area and therefore, many studies have been done to improve its properties by combination with other oxides. Alumina-ceria is substantial component of the three ways catalysts, due to the ceria ability to function as the buffer of oxygen and to enhance the oxygen storage capacity of the catalysts. Ceria in these catalysts also functions as structural promoting component, increasing alumina stability towards thermal sintering. Promising method of oxides preparation, very interesting and simple but not sufficiently studied yet is a mechanochemical synthesis. Here we report on the synthesis of nano-sized alumina, ceria and ceria-alumina of various compositions by a wet solid phase mechanochemical reaction of hydrous aluminum, and/or cerium nitrate with ammonium bicarbonate after addition of a small amount of water. The aim of this contribution is to study processes being in progress during synthesis of the mixed oxides, interaction between components and their mutual effect on the properties of resulting products. The phase evolution during mechanical milling and the subsequent heat treatment of precursors were studied by X-ray diffraction, DTA/TG, H_2-TPR, NH_3-TPD, CO_2-TPD, N_2 adsorption at -195°C, IR, and XPS spectroscopy. Alumina and mixtures of alumina with different quantities of CeO_2 (1- 18 wt. %) were synthesized by mechanochemical method from aluminum nitrate, cerium nitrate and ammonia bicarbonate.

Experimental

Al, Al-Ce and Ce oxides preparation

Aluminum oxide and aluminum/cerium mixed oxides were prepared by mechanochemical process from aluminum nitrate or from both aluminum and cerium (III) nitrate $Ce(NO_3)_3.6H_2O$ used in various proportions. The aluminum nitrate was first fused (m.p. 72.8°C) and after addition of NH_4HCO_3 at 80 °C the mixture was grinded in an agate mill for 1 h. The reaction product was dried 20 h at 60°C and calcined 4 h at 500°C. Mixed aluminum-cerium and cerium oxide precursors were prepared similarly: $Ce(NO_3)_3.6H_2O$ was slowly added to the fused aluminum nitrate and then, NH_4HCO_3 was added at 60°C; the mixture was grinded and further treated as described above. The products were labeled by the number of intended CeO_2 amount (wt. %) in the resulting oxides, e.g. Al_2O_3-18CeO_2.

Content of cerium in the calcined precipitates was determined by chemical analysis using ICP-AES after dissolution of the samples in water solution of HCl.

Surface area was determined by nitrogen physisorption at -195°C using Micromeritics ASAP 2010 after drying the samples at 105°C and evacuating at 350°C (approximately 2–5 h).

Thermogravimetry (TG) and differential thermal analysis (DTA) of the selected dried samples were performed using a Setaram Setsys Evolution instrument. The heating rate 10°C min^{-1}, air-flow rate of 75 ml min^{-1} and 20-mg samples were used for the measurements. In the separate instrument equipped with a quadrupole mass spectrometer OmniStar (Pfeiffer Vakuum) the analysis of gaseous product evolving during calcination of the dried precipitates was performed under identical conditions as TG measurements were done. Gaseous products were continuously monitored for the mass numbers *m/z* (*16*-NH_3^+, *18*-H_2O^+, *30*-NO, *44*-CO_2).

X-Ray measurements were performed using a Philips X´pert PW3020 instrument, equipped with a Cu Kα Bruker AXS 2D Powder X-Ray analyzer with filtered $CuK\alpha_1$ radiation (λ=0.154056 nm), a graphite monochromator, and rate of 0.01° per 0.5 s.

Infrared spectra of the samples mixed with KBr at approximately 0.5 wt% concentration were recorded on a Nicolet Impact 400 FTIR spectrophotometer (Thermo Electron Corporation, USA). The spectra were taken in the region of 4000-400 cm^{-1} at 0.4 cm^{-1} resolution using 100 scans. Alumina absorption in the 400-1200 cm^{-1} range was compensated by subtraction of a normalized spectrum of the equivalent amount of support from the spectra of the catalysts.

Temperature-programmed reduction (H_2-TPR) of the calcined samples (0.025 g) were accomplished with an H_2/N_2 mixture (10 molar% of H_2) and a flow rate of 50 ml min^{-1} with a linear temperature increase of 20 °C min^{-1} up to 1000 °C. During the TPR measurement, the change in composition of H_2/N_2 mixture was recorded by catharometer. Reduction of the grained CuO (0.16-0.315 mm) was performed to calculate the absolute values of the hydrogen consumed during the reduction.

Temperature-programmed desorption of NH_3 and CO_2 (NH_3-TPD, CO_2-TPD) was accomplished with a 0.050 g sample at 20-1000°C with a helium carrier gas and NH_3 or CO_2 as an adsorbing gas. Ten doses (912 µl each) of

NH_3 (or CO_2) were applied to the catalyst sample at 30°C before flushing of the sample with helium for 1 h and heating with ramp rate 20°C min^{-1}. The mass contributions (*m/z*) *16*-NH_3^+ or *44*-CO_2 was collected using an Omnistar mass spectrometer (Pfeiffer Vakuum).

XPS measurements were performed with an ESCALAB-Mk II (VG Scientific) electron spectrometer with a base pressure of ~5.10^{-8} Pa. The samples were excited with AlKα radiation (hν=1486.6 eV). The total energy resolution of the instrument was 1.2 eV as measured by the FWHM of the Ag 3d5/2 photoelectron line. The following photoelectron lines were recorded: C 1s, O 1s, Al 2p, Ce $3d_{3/2}$, and Ce $3d_{5/2}$. All binding energies were related to the C 1s photoelectron line centered at 285.0 eV. The surface atom concentrations were evaluated using the photoelectron peak areas divided by the corresponding sensitivity factors taken from[1].

Results and discussion

In addition to pure alumina and ceria, eight alumina-ceria mixed oxides samples with various CeO_2 and Al_2O_3 concentrations were prepared mechanochemically. Concentration of cerium oxide in the alumina samples varied from 0.05 to 18 wt. %. Small deviation of the real CeO_2 concentrations from the intended was found which could be accounted to inaccuracies caused by losses during samples preparation.

The precipitates produced by mechanochemical reaction of the corresponding nitrates with NH_4HCO_3 differed in dependence on their composition. In case of Al and Al-Ce nitrates, the use of ammonium bicarbonate as a precipitating agent resulted in a voluminous white precipitates, while yellowish precipitate was obtained in case of Ce(III) nitrate. SEM images of the Al ions precipitate, of the mixed Al-Ce precipitate having 18 wt. % CeO_2 and Ce ions precipitate prepared mechanochemically showed that dried alumina precipitate consists of nearly spherical particles, while pure Ce precipitate formed substantially larger platelets. The shape of the particles and sizes of the mixed Al_2O_3-$18CeO_2$ sample resembled that of pure alumina precipitate. The finding is in accord with the data published by Djuricic and Pickering[2] who found that amorphous precipitates such as aluminum hydroxide consisted of spherical particles whereas crystalline precipitates often conatined faceted particles. Agglomeration of primary particles of amorphous precipitate in a suspension usually proceeds to form densely packed agglomerates. The agglomerates often have a narrow size distribution and tend to be spherical when the precipitates were amorphous. Agglomerate diameters up to 1 micron are frequently obtained. Akinc and Sordelet[3] and Chen and Chen[4] prepared non-spherical well-crystalline $Ce(OH)CO_3$ microplates as the precursor particles. The shape of the $Ce(OH)CO_3$ microplate was sustained[5] after thermal decomposition/oxidation to CeO_2.

Crystal structure and phase identification of the mechanochemically prepared precursors, dried at 60°C, are analyzed from the X-ray diffraction patterns. Fig. 1 shows diffraction lines of three samples: a) alumina with low amount of cerium (sample Al_2O_3-$0.05CeO_2$), b) Al_2O_3-$18CeO_2$ and c) pure CeO_2. Diffraction lines of the alumina precursor show peaks indicating rather low crystallinity of the sample. The main component is aluminum ammonium carbonate hydroxide $NH_4Al(OH)_2CO_3$ (PDF 71-1314), accompanied with a rest of unwashed ammonium nitrate (PDF 01-0809). The main chemical reaction of Al nitrate precipitation can be written as follows[6]:

$$Al(NO_3)_3+4NH_4HCO_3 \rightarrow NH_4AlO(OH)HCO_3\downarrow+3CO_2\uparrow+H_2O+3NH_4NO_3$$

XRD analysis of the Al_2O_3-$18CeO_2$ precursor indicated that presence of ceria in the amount of 18 wt% led to formation of less crystalline precipitate than pure alumina precursor. In the precipitate, aluminum ammonium carbonate hydroxide $NH_4Al(OH)_2CO_3$ in the highest extent was found together with aluminum hydroxide gibbsite $Al(OH)_3$ (PDF 07-0324). Cerium in the precipitate appeared as cerium nitrate hydrate $Ce(NO_3)_3.5H_2O$ (PDF 22-0544).

XRD analysis of the dried Ce precipitate prepared by milling of Ce nitrate with ammonium bicarbonate revealed somewhat complicated picture. Following compounds containing cerium were identified: cerium carbonate hydroxide $Ce(OH)CO_3$ (PDF 41-0013), cerinite $Ce_2(CO_3)_3.6H_2O$ (PDF 30-0295) and a small amount of cerium hydroxide $Ce(OH)_3$ (PDF 74-0665). Unfortunately, the peak found at 2ϑ=8.170° having the highest intensity and the peak at 2ϑ=18.4° was not possible to classify even using the XRD database from the 2011 year. All cerium compounds recognized in the dried precipitate occur in the (III) oxidation state and therefore, oxidation of Ce^{3+} to Ce^{4+} during precursor preparation did not take place like in case of precipitation of Ce nitrate with ammonium hydroxide at high pH values[2]. XRD analysis revealed no compounds containing nitrogen in this dried precipitate.

IR spectra of the dried precipitates confirmed presence of all ions in the compounds mentioned above. The large band centered at 3500 cm^{-1} is assigned to the O-H stretching modes of interlayer water molecules and of H-bound OH groups, and the peak at 1630 cm^{-1} is due to the bending mode of water molecules[7]. Intensities of the peaks are higher in the spectra of the samples containing alumina. Four weak bands at 850, 1100, 1354, and 1450 cm^{-1} are characteristic of carbonate ions[8]. Three of them are visible in the spectra, only the band at

1354 cm^{-1} is overlapped by the peak with maximum at 1380 cm^{-1} ascribed to NO_3^- ion. Presence of NH_4^+ ions in the solid samples is documented[9] by the peak centered at 3150 cm^{-1} and at 1430–1390 cm^{-1}. The highest concentrations of NH_4^+ ions are observed in the samples in which aluminum ammonium carbonate hydroxide was identified. Ce precipitate showed the least concentration of ammonium ions, very likely, incorporated in the compound non-identified by XRD. After calcination of the as-prepared samples at 500 °C, poor peaks indicating low crystallinity of the high-concentrated alumina samples were observed (Fig. 2). Formation of the gamma- and/or eta-alumina could be assumed[11] in the calcined alumina precursor

$NH_4AlO(OH)HCO_3\downarrow \rightarrow CO_2+H_2O+AlOOH + NH_3$.

As the cubic gamma-alumina (PDF 50-0741) and eta-alumina are hardly distinguishable, it cannot be surely concluded which of these two alumina phases are present in the examined catalysts. X-ray diffraction peaks at 28.54, 33.17, 47.462 and 56.278, characteristic of CeO_2 in cubic fluorite structure (JCPDS data file 34-0394, 43-1002) and clearly seen in the XRD spectrum of the pure CeO_2 sample (Fig. 2) are in good agreement with the data (28.58, 33.38, 47.58 and 56.48°) published previously[11,12].

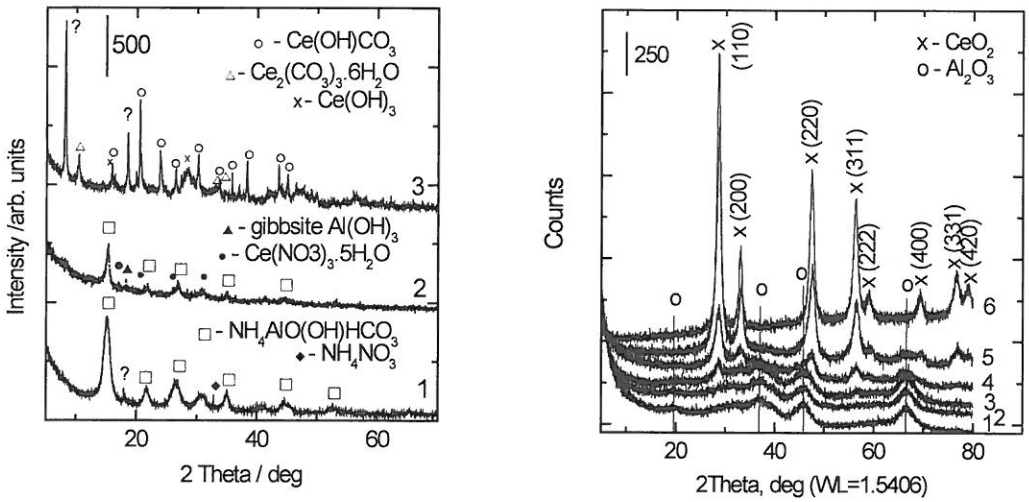

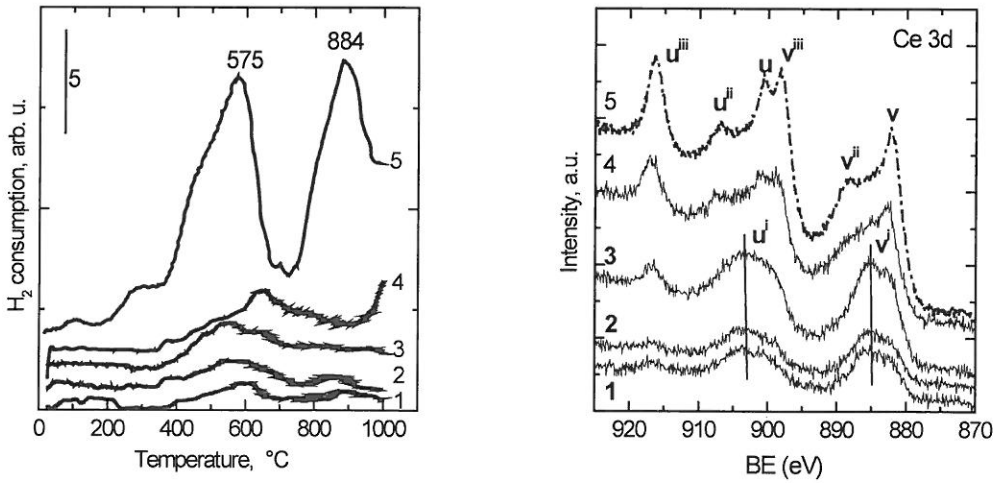

Figure 1. XRD patterns of the precursors: 1: Al_2O_3-0.5CeO_2, 2: Al_2O_3-18CeO_2, 3: CeO_2

Figure 2. XRD patterns of the calcined precursors. 1: Al_2O_3, 2: Al_2O_3-0.5CeO_2, 3: Al_2O_3-1.5CeO_2, 4: A_2O_3-4CeO_2, 5: Al_2O_3-10CeO_2, 6: CeO_2

Figure 3. TPR profiles of the calcined precursors. 1: Al_2O_3-0.5CeO_2, 2: Al_2O_3-1.5CeO_2, 3: A_2O_3-4CeO_2, 4: Al_2O_3-10CeO_2, 5: CeO_2

Figure 4. XPS spectra of Ce 3d core electron levels for the calcined precursors. 1: Al_2O_3-0.05CeO_2, 2: Al_2O_3-1.5CeO_2, 3: A_2O_3-4CeO_2, 4: Al_2O_3-10CeO_2. Dashed line corresponds to bulk CeO_2.

In the mixed Al_2O_3-CeO_2 samples, the presence of nanocrystalline phase, cubic CeO_2 (cerianite), is confirmed by (111) reflection at 2θ =33.3°. Other intense CeO_2 reflections (200 and 311) cannot be found because they are either not present or overlapped by γ-alumina (220) and (422) reflections. d-Spacing of Al_2O_3 planes (Table 2) gradually decreases with increasing amount of ceria added to the alumina and is the lowest for the sample containing 10 wt. % CeO_2. The value found for pure ceria is higher than that for the mixed Al-Ce oxides but lower than for pure alumina. In contrast to Sasikala et al.[13], formation of $CeAlO_3$ was not observed by XRD. The finding is very likely connected with high dispersion of Al_2O_3 in which cerium is included. $CeAlO_3$ could exist as a dispersed phase where Ce^{4+} is stabilized in cation vacancies on the alumina surface or is inserted and forms solid solution. Presence of CeO_2 in alumina stabilizes its structure. Very likely, cerianite starts nucleating at the defects of oxygen (oxygen vacancies) forming bridges with O_2 between Al_2O_3 and CeO_2 saving alumina structure, as Ce^{4+} (ionic radius Ce^{4+}=0.092 nm) can substitute Al^{3+} (ionic radius Al^{3+}=0.051 nm) in Al_2O_3 structure. CeO_2 continues to grow with its increasing content in alumina forming bulk cubic CeO_2 nanocrystals[14].

Thermogravimetric mass-loss measurements accompanied with mass spectrometry of effluent of the three selected precursors, Al_2O_3-0.05CeO_2, Al_2O_3-18CeO_2, and CeO_2 were done to find temperature ranges in which transformation of the precursor proceeds. Transformation of the dried Ce precipitate proceeded in the narrow temperature range 194-275°C. In these temperatures, substantial part (26.3 %) of the total weight loss (35.6 %) was realized. Maximum rate of the weight loss caused by exothermic reaction, probably decomposition of ammonium nitrate, was found at T_{max}=206°C. In the gas effluent formed at 170 °C, the mass spectrometer detected masses *m/z 16* (NH_3), *18* (H_2O), *30* (NO), and *44* (CO_2). The findings indicate that apart from sample dehydration, decomposition of carbonates e.g. cerium carbonate hydroxide $Ce(OH)CO_3$ and/or cerinite $Ce_2(CO_3)_3.6H_2O$ proceeds. Appearance of ammonia in the effluent reveals presence of small amount of ammonium salts in the precursor, e.g. NH_4NO_3. In contrast to relatively simple process of thermal transformation of the Ce precursor, the alumina sample containing negligible amount of CeO_2 (Al_2O_3-0.05CeO_2) showed behavior that is more complex. Dehydration of the sample was in progress at 71 °C what is proved by 9 % of weight loss and presence of the gas with *m/z*=18 in this DTG peak. Two maxima of H_2O appearance were observed in the effluent at 222 and 285 °C connected with the loss of water produced by dehydroxylation of the hydroxides. Another 33.5 % of mass loss was observed in this temperature range. As ammonia was detected in the effluent in the first peak (T_{max}=222 °C), decomposition of aluminum ammonium carbonate hydroxide $NH_4Al(OH)_2CO_3$, found in the dried precipitate by XRD, has to proceed. In the second peak of the effluent, CO_2 (*m/z*=44) was identified, and therefore, carbonates are decomposed. Mass spectroscopy also identified some amount of NO (temperature range 250–550 °C) arising due to decomposition of nitrate ion.

TG/DTA analysis of the sample containing 18 wt% CeO_2 resembles the analysis of the pure alumina sample with some marks of CeO_2 analysis. Up to 152 °C, weight loss 22.6 % was found, and another 22.2 % was observed up to 227 °C. The rest of 9.6 % of weight loss was observed up to 868 °C. Two main endothermic peaks with T_{max} 139 and 206 °C correspond to dehydroxylation and decomposition of aluminum ammonium carbonate hydroxide $NH_4Al(OH)_2CO_3$. Nitrates in cerium nitrate hydrate $Ce(NO_3)_3.5H_2O$ could be decomposed in higher temperature range with T_{max}=282 °C.

Porous structure measurement of the calcined precipitates confirmed high surface area (Table I) of the pure aluminum oxide (285 m^2g^{-1}). Increasing amount of ceria in the mixed alumina-ceria resulted in a gradual, non-linear decrease in the surface area, pure ceria surface area being the lowest (70 m^2g^{-1}). The observed decrease in the surface area with increasing concentration of ceria does not correspond with the weight parts of both components (alumina and ceria) in the mixed oxides, as the decrease in the mixed oxides surface area is more substantial. The phenomenon can be likely caused either by formation of a new compound based on alumina-ceria or by changes in primary particles size. Volume of micropores gradually decreased with increasing ceria concentration in the Al-Ce mixtures from 52 mm^3g^{-1} (calcined aluminum oxide) to 13.8 mm^3g^{-1} (ceria). The findings are very likely connected with the size of primary particles. The micropores are formed in the space among the smaller primary particles and these were found in the samples with high concentration of aluminum hydroxide. A larger space among the larger platelets of dried Ce precipitates exists and therefore, larger diameter of pores can be observed. Volume of mesopores, similarly as the average diameter of pores, did not change substantially with the varying composition of the supports.

Table I
Amount of CeO_2, crystalline phase in the precursors, lattice parameter *d* of the cubic oxides and characteristic values of porous structure of the calcined Al-Ce mixed oxides

Sample	CeO_2 [wt.%]	Crystalline phase [%]	d [nm]	S_{BET} [m^2g^{-1}]	V_{meso} [cm^3g^{-1}]	V_{micro} [mm^3g^{-1}]	D [nm]
Al_2O_3	0.01	Amorphous	1.9835	285	0.56	52.2	6.7
Al_2O_3-0.05CeO_2	0.05	23.4	1.9770	259	0.56	47.2	7.6
Al_2O_3-1.5CeO_2	1.74	23.5	1.9641	285	0.53	50.1	6.3
Al_2O_3-4CeO_2	4.09	36.5	1.9100	237	0.52	45.5	7.8
Al_2O_3-10CeO_2	10.5	63.3	1.9048	169	0.44	30.0	8.8
CeO_2	100	74.3	1.9142	70	0.15	13.8	5.8

$D=4V_{meso}/S_{BET}$

IR spectra of the prepared oxides, excluding spectrum of CeO_2, revealed very similar picture. Broad absorption in the region 450–800 cm^{-1}, characteristic of the gamma-Al_2O_3 phase[15], was detected in the spectrum of the synthesized alumina. The band with maximum at 1120 cm^{-1} is connected with the deformation vibrations of OH^- groups on the Al_2O_3 surface. Absorption in the region 450-800 cm^{-1} was significantly increased in the sample containing 0.5 and 1.5 wt. % CeO_2 and this band could be connected with formation of Al-O aluminate bond. In the spectrum of the sample having substantially higher concentration of CeO_2 (Al_2O_3-10CeO_2), the band at 670 cm^{-1}, observed in the spectrum of the pure CeO_2, was also seen. In the literature, the band at 700 cm^{-1} was observed in IR spectrum of pure ceria, and it was ascribed to the envelope of the phonon band of the metal oxide (CeO_2) network[16]. The shift in the band position can be caused by different procedure of the sample preparation. Decrease in the intensity of the 1120 cm^{-1} band with increasing concentration of CeO_2 in the mixed oxides permits to suggest that this phase, lowering the number of surface Al-OH groups, is present on the sample surface. The bands around 1170–1000 and 960–850 cm^{-1} could be associated with the formation of „carbonate-like" species on the ceria surface[17].

Temperature programmed reduction patterns of the synthesized oxides are presented in Fig. 3. Two main reduction regions are observed in the TPR profile of CeO_2. The two principal regions appear at 300-600 °C with T_{max} 520-550 °C and at 750-1000 °C with T_{max} around 850 °C. The two reduction regions are characteristic of ceria reduction and they are attributed to the reduction of Ce^{4+} to Ce^{3+} (maximum at about 525 °C) and bulk ceria reduction (maximum at 875 °C), respectively[18,19]. In the literature, following reduction maxima can be found in the TPR profiles for ceria: two main reduction peaks at 577 and 886 °C together with a shoulder at 269 °C. The shoulder at 269 °C can be attributed to the reduction of surface cerium oxide[18] and thus, it corresponds to the reduction of Ce^{4+} to Ce^{3+}. The peak at 577 °C is ascribed to reduction of CeO_2, for this peak was identified as the main peak in the TPR profiles of CeO_2–Al_2O_3 supports with different CeO_2 loading after calcination at 500 °C[12]. The peak observed at 438 °C was attributed to the reduction of surface cerium oxide[20]. The peak at 560 °C was ascribed to the reduction of bulk CeO_2; this peak was identified as the main peak in the TPR profiles of CeO_2–Al_2O_3 supports with different CeO_2 loading and calcined at 500 °C[21].

High mobility of surface oxygen species in ceria is known, and for that reason, oxygen can be removed under reduction atmosphere forming[22] non-stoichiometric ceria CeO_{2-x}. At low temperature, the surface oxygen ions can be removed more easily than bulk oxygen, which requires transportation to the surface before reduction. The TPR results show that the major part of oxygen ions in the Al-Ce mixed oxides is more mobile than those in the pure CeO_2 are, as the reduction process proceeds more easily, i.e. at lower temperatures. The shift of the reduction peaks to lower temperature indicates interaction between the oxides in their mixture. Only the sample with 18 wt. % CeO_2 is reduced with more difficulty than the other samples (Fig. 3). The phenomenon could be connected[23] with partial reduction of Ce^{4+} to Ce^{3+}during precursor decomposition in the stage of its calcination $Ce\text{-}(H_2O) \rightarrow Ce^{3+}\text{-}OH + H^+$.

The obtained reduction curves were integrated in two temperature ranges, the first one being 25–500 °C (interesting for catalytic reactions), the second one 25-1000 °C. The highest amount of hydrogen consumed in the temperature range 25–500 °C was found with pure ceria (0.48 mmol g^{-1}), while the lowest one (0.08 mmol g^{-1}) showed the sample with the lowest concentration of ceria. In accord with expectation, the mixed Al-Ce oxides samples showed reducibility within these two limits.

NH_3-TPD of the calcined precipitates proceeded in the temperature range of 25–350 °C only. It indicates that the oxides do not comprise very strong acidic sites. The principal part of the sites can be ascribed to the sites of very low acidity with a distinct desorption peak at about 60 °C. Low acidity was also observed in case of pure alumina, which comprises, apart from very weak sites, slightly stronger sites appearing as a shoulder at about

148 °C. The shoulder decreases with increasing amount of CeO_2. Acidity of the pure alumina was lower (0.28 mmol g^{-1}) than that observed with Sasol alumina (around 0.35 mmol g^{-1}) prepared by other method. Increasing concentration of ceria in alumina led to decreased amount of the sites with low acidity. Basicity of all prepared samples determined by CO_2-TPD was in all cases higher than their acidity. The amount of basic sites in alumina-ceria samples increased with increasing amount of ceria in the samples. Pure ceria showed, however, lower basicity than that of the mixed Al_2O_3-10CeO_2 sample. This finding is in accord with its higher acidity.

XPS spectra of Ce 3d core electron levels for Al_2O_3-CeO_2 mixed oxides with varying CeO_2 loadings after calcination at 500°C are shown in Fig. 4. The XPS spectrum of bulk CeO_2 is complex, consisting of six components, corresponding to three pairs of spin-orbit doublets: ***v*** represents the Ce $3d_{5/2}$ contribution, and ***u*** represents the Ce $3d_{3/2}$ contribution[24]. It is seen that XPS spectra of the Al_2O_3-CeO_2 mixed oxides are different from that of the pure CeO_2, and depend on the CeO_2 loading. The broadening of the XPS lines for oxide samples suggests the presence of several surface cerium oxide species; a new weak band (v^i) at about 885.4 eV appears in the samples with 0.5-4 wt% CeO_2. The increasing intensity of the v^i band and disappearance of v^{ii} with increasing CeO_2 loading (up to 4 wt. %) points out that cerium at low content (0.5-4 wt. %) is in a reduced state (III). In addition, it should be noted that some photoreduction of Ce^{4+} might take place during exposure of the samples to a high X-ray flux under ultra-high vacuum employed during data acquisition. It is seen in Fig. 4 that the intensity of u^{iii} increases with increasing CeO_2 loading, what means an increase in the relative amount of Ce(IV). We can thus conclude that the Ce^{4+}/Ce^{3+} redox couple exists on the surface of the Al_2O_3-18CeO_2 mixed oxide. It should suggest formation of CeO_2 crystallites, whose presence were proved by XRD in this sample. The XPS atomic ratios of Ce/(Ce+Al) for the calcined mixed oxides are listed in Table II. The data demonstrate that

Table II
Surface concentrations of Al, O and Ce (at%) in the Al_2O_3-CeO_2 mixed oxides

Sample	Al 2p	O 1s	Ce 3d	Ce/(Ce+Al)[a]	Ce/(Ce+Al)[b]
Al_2O_3	36.23	53.72	0	0	0.000
Al_2O_3-0.05CeO_2	35.72	52.06	0.19	0.005	0.0001
Al_2O_3-1.5CeO_2	36.15	53.02	0.25	0.007	0.005
Al_2O_3-4CeO_2	35.58	52.93	0.40	0.011	0.012
Al_2O_3-10CeO_2	36.35	54.08	0.64	0.017	0.034
CeO_2	0	48.64	18.85	1	1.000

[a] Atomic ratio calculated from XPS, [b] Atomic ratio based on chemical analysis

the Ce/(Ce+Al) ratios in surface layers increase with increasing CeO_2 loading. Surface concentration of cerium is higher than concentration in bulk for the samples having low cerium concentration (< 4 wt. %). With increasing CeO_2 loading bulk concentration is higher than the surface what confirms formation of separated CeO_2 crystallites in the calcined precipitates.

Conclusions

Pure alumina, pure ceria and mixtures of both oxides having 0.05 up to 18 wt. % CeO_2 were prepared mechanochemically from aluminum and/or cerium nitrates with ammonia bicarbonate. Aluminum ammonium carbonate hydroxide $NH_4Al(OH)_2CO_3$ was found to be main product in the dried Al precipitate, while cerium carbonate hydroxide $Ce(OH)CO_3$ was prevailing in the dried Ce precipitate. After calcination at 500 °C, amorphous structure of alumina and cubic fluorite crystallites of ceria with preferred orientation along (1 1 1) direction were detected by XRD. XPS spectrum confirmed the existence of Ce^{4+} oxidation states in the calcined mixed oxides when concentration of CeO_2 is higher than 6 wt. %. Surface acidity of the mixed oxides prepared mechanochemically is lower than that observed at oxides prepared by other methods because of presence of adsorbed ammonia on the surface. IR spectroscopy results are in accord with the findings. Addition of CeO_2 to alumina slightly decreases surface area and mesopore volume of the resulting mixed oxides. Surface concentration of Ce in the mixed Al-Ce oxides increases faster with increasing bulk Ce concentration than could be expected from the data of chemical analysis. The reason is likely the insertion of Ce ions into the Al_2O_3 lattice.

Mechanochemical procedure of the Al-Ce mixed oxide preparation is relatively simple and facile which does not produce large quantities of wastewaters influencing unfavorably the life environment. Moreover, due to the use of initial reactants (nitrates and ammonium salt) the products do not contain sodium, which is very often not advantageous in catalytic supports. The products are suitable as supports of heterogeneous catalysts for hydrodesulfurization reactions or directly as catalysts for total oxidation reactions.

Acknowledgment

This work was carried out in the framework of bilateral Czech-Bulgarian scientific cooperation and was supported by Czech Science Foundation (grant GA 14-13750S).

Literature

1. Scofield J.H.: J Electron Spectrosc. Relat. Phenom. *8*, 129 (1976).
2. Djuricic B., Pickering S.: J. Euro. Ceram. Society *19*, 1925 (1999).
3. Akinc M., Sordelet D.: Adv. Ceram. Mat. *2*, 232 (1987).
4. Chen P.L., Chen L.W.: J. Am. Ceram. Soc. *76*, 1577 (1993).
5. Guo Z., Du F., Li G., Cui Z.: Inorg. Chem. *45*, 4167 (2006).
6. Zhisen Wu, Youde Shen, Yan Dong, Jianqing Jiang: J. Alloys Comp. *467*, 600 (2009).
7. Zhu Y., Li H., Koltypin Y., Gedanken A .: J. Mater. Chem. *12*, 729 (2002).
8. Labajos F.M., Sastre M.D., Trujillano R., Rives V.: J. Mater. Chem. *9*, 1033 (1999).
9. Nakanishi Koji, Solomon P.H.: *Infrared Absorption Spectroscopy,* 2nd edn., Holden-Day Inc., San Francisco, 1977.
10. Wefers K., Misra Ch.: Technical Report No. 19 Revised. Alcoa Laboratories (1987).
11. Fathi M., Bjorgum B., Viig T., Rockstad O.N.: Catal. Today *63*, 489 (2000).
12. Santos A.C.S.F., Damyanova S., Texeira G.N.R., Mattos L.V., Noronha F.B., Passos F.B., Bueno J.M.C .: Appl. Catal. A *290*, 123 (2005).
13. Sasikala R., Sudarsan V., Kulshreshtha S.K: J. Solid State Chem. *169*, 113 (2002).
14. Jun Fang, Xinzhen Bi, Dejun Si, Zhiquan Jiang, Weixin Huang: Appl. Surf. Sci. *253*, 8952 (2007).
15. Uvarov A.V., Antipina T.V., Tihomirova S.P.: Zhur. Fiz. Khim. (Rus) *41*, 3059 (1967).
16. Zawadzki M.: J. Alloys Comp. *454*, 347 (2008).
17. Suresh R., Ponnuswamy V., Mariappan R.: Appl. Surf. Sci. *273*, 457 (2013)
18. Ranga Rao G., Mishra B.G.: Bull. Catal. Soc. India *2*,122 (2003)
19. Martin D., Duprez D.: J. Phys. Chem. *100*, 9429 (1996).
20. Bernal S., Calvino J.J., Cauqui M.A., Gatica J.M., Larese C., Perez-Omil J.A., Pintado J.M.: Catal. Today *50*, 175 (1999).
21. Trovarelli A., Dolcetti G., Leitenburg C., Kaspar J., Finetti P., Santoni A. : J. Chem. Soc. Faraday Trans. *88*, 1311 (1992).
22. Hardacre C., Ormerod R.M., Lambert R.M.: J. Phys. Chem. *98*, 10901 (1994).
23. Araujo A.S., Aquino J.M.F.B., Souza M.J.B, Silva A.O.S.: J. Solid. State Chem. *171*, 371 (2003).
24. Burroughs P., Hamnett A., Orchard A.F., Thornton G.: J. Chem. Soc. Dalton Trans. *17*, 1686 (1976).